Available online at www.sciencedirect.com
SCIENCE DIRECT®
C. R. Physique 7 (2006) 198–212
COMPTES RENDUS PHYSIQUE
http://france.elsevier.com/direct/COMREN/

High power fiber lasers and amplifiers/Lasers et amplificateurs à fibre de puissance

Fiber lasers integration for *LMJ*

Alain Jolly *, Jean-François Gleyze, Denis Penninckx, Nicolas Beck, Laurent Videau, Hervé Coïc

CEA, centre d'études scientifiques et techniques d'Aquitaine, 33114 Le Barp, France

Available online 6 March 2006

Abstract

The Fibre-Injection System in the *LIL–LMJ* facilities makes use of a single-mode fiber based arborescent architecture. Starting from a unique single-mode oscillator, it consists of a high performance *PM* design which is dedicated to the generation of pulses onto a large number of synchronous outputs. The optical features to be optimised involve dynamic ranges in excess of 50 dB and the generation of 25 ns wide arbitrary waveforms at 100 ps time resolution, of which the *PSD* looks like a precisely controlled Bessel distribution. We analyse the complete design issues, together with the optical components which have been developed specifically. ***To cite this article: A. Jolly et al., C. R. Physique 7 (2006).***

Résumé

Intégration des lasers à fibre pour le *LMJ*. Le dispositif d'injection optique pour l'équipement des grandes installations laser pour la fusion s'appuie sur une architecture arborescente à base de fibres monomodes. A partir d'un oscillateur monomode continu, unique et couplé à une structure à maintien de polarisation, un grand nombre d'impulsions sont générées sur autant de sorties synchrones après avoir été mises en forme. L'optimisation des performances optiques nécessite de maîtriser la dynamique en intensité dans une gamme de valeurs étendues sur plus de 50 dB. Les profils des impulsions, de forme arbitraire à l'intérieur d'une fenêtre de durée 25 ns, sont définis avec une résolution temporelle de 100 ps. La densité spectrale de puissance présente la forme d'une distribution de raies de Bessel contrôlées de manière très précise. Nous présentons les principaux éléments de dimensionnement et les composants développés dans la version actualisée du dispositif. ***Pour citer cet article : A. Jolly et al., C. R. Physique 7 (2006).***

Keywords: Fibre amplifiers; Polarisation maintaining; Phase modulation; Pulse shaping

Mots-clés : Amplificateurs fibrés ; Maintien de polarisation ; Modulation de phase ; Mise en forme temporelle

1. Fusion requirements and related laser features

This article deals with an update of the integration of fibre-coupled lasers which are involved in the pulse generation on large-scale laser facilities dedicated to the process of Inertial Confinement Fusion (*ICF*) in France [1–3]. The two involved programs consist of the Ligne d'Intégration Laser (*LIL*) and the Laser Mégajoule (*LMJ*), under construction

* Corresponding author.
E-mail address: alain.jolly@cea.fr (A. Jolly).

1631-0705/$ – see front matter
doi:10.1016/j.crhy.2006.01.017

today. The LIL project is a full-scale demonstrator (8 beam lines) to validate the LMJ (240 beams lines). The current technological options [4,5] for the design of the so-called Fibre Injection Systems (*FIS*) first attempt to take advantage of the advances from the R&D in the field of telecommunications each time this is possible, together with specific insights in electro-optics when required. It must be underlined that an *ICF* application implies a number of specific requirements: first, the working wavelength needs to match the peak of fluorescence in Neodymium doped phosphate glasses, i.e., our working wavelength will be $\lambda_o = 1053.00$ nm. Phosphate glasses are the only materials to be available for very large size laser amplifiers, in the range of tens of centimetres wide optical apertures. As a result, the guided-wave and fibre-coupled optical components can not be founded in the standard catalogues of telecommunication networks. They have to be re-designed specifically. Second, the feeding of the laser systems downstream requires very high optical contrasts, in excess of 50 dB, using a few nanosecond wide pulses of which the intensity dynamic range has to be higher than 30 dB. As it will be shown in the article, the involved peak powers vary from about 10 mW to more than 10 W along the structure of the *FIS*, in order to finally provide about 100 mW per single output. At least we also need to couple to what basically consists of a Single-Mode (*SM*) configuration, specific phase and intensity modulations to operate the laser facility on an efficient and reliable way. Both kinds of modulations should remain fully uncoupled anywhere in the system. When combined, such issues imply to consider the usual telecom approaches in another light and define some unusual optical tradeoffs for the optimization of the output performance. Even though the *FIS* consists of a small size and relatively low cost part in the facility, its contribution to the overall laser performance will be of prime importance.

From a general point of view, to reach fusion by the *ICF* process with the help of a laser, one has to manage a number of operations such as precise pulse shaping and synchronization, a good target balance and spatial uniformity in the target plane, together with energy production at the allowed highest beam intensities. We will start this update on the design of the *FIS* by the optical functions to provide and the system's architecture. Then, we will go on with the description of the optical components before to end with the main issues related to the management of the output performance and a perspective.

2. A number of optical functions to be implemented within an arborescent fibre-coupled architecture

2.1. Operational features for ICF

Fusion lasers always consist of highly modular designs, due to the huge numbers of amplifying beam sections required for the production of Méga-joule energies. The *LMJ* will consist of 240 independent beam sections to be packed by four units (quads). Each section has to provide up to 20 MJ of infrared energy within a unique pulse of which the typical width is 4 ns. To generate such an amount of output energy each beam section is fed with up to nearly 1 J input energy, using a Pre-Amplifier Module (*PAM*). The *PAM* itself, which is, in other respects, the location where the single laser beam acquires its squared near field shape [4], is fed with the help of a single output from the *FIS*, of which the pulse energy ranges from 0.1 to 1 nJ.

The purpose of Single-Mode injection is to get free from any uncontrolled intensity-modulation. In the presence of mode-beating effects due to multimode configurations, and using the definition of a ratio of the half peak-to-peak value to the mean power value, the relative amplitude of these modulations is 100%. Even though they can not be resolved properly versus time or space, such effects are quite deleterious for the management of the optical damage effects in the final optics of *ICF* lasers, at very high optical intensities.

One or two Phase-Modulations have to be operated inside the *FIS*, versus the expected lightning configuration on the target. If operated simultaneously, they will always remain asynchronous and truly independent. The first ($P_h M_{SBS}$) is related to the suppression of Stimulated Brillouin Scattering effects (*SBS*), to benefit from the highest attainable laser intensity at the output of the facility. It can never be disconnected, and some failure should be dramatic for the complete facility. The second helps to compensate for a drawback of highly coherent laser designs, namely the deleterious effects of the laser speckle on to an *ICF* target. The speckle produces a small scale non-uniform irradiance distribution, which may prevent an efficient compression. So, the degree of coherence needs to be lowered in the system. This is the reason why another specific Phase-Modulation ($P_h M_{SSD}$) can be required, to make use downstream of precisely controlled light diffraction effects at wavelength dependent angles. This process [6] consists of optical smoothing, or Smoothing by Spectral Dispersion (*SSD*), by the way of a precisely controlled Power Spectral Density (*PSD*) to be generated inside the *FIS*. Under the assumption of temporal modulations to be kept fast enough

with respect to the pulse width, the process of *SSD* couples the phase variations to dispersion effects. When the Phase-Modulated beam crosses dispersive optical components downstream such as phase plates and gratings, there exist periodic deviations along the longitudinal and/or transverse directions. As a result, the distribution of the speckle on the target experiences a rapid shifting, at the frequency of the $P_h M_{SSD}$. This way, the time-integrated spot density looks more uniform. When defined by its integrated value during the whole pulse width, by the ratio of the local peak-to-peak fluctuations of the local power within the section of the beam to its averaged value of power, the optical contrast then decreases from 100% down to about 10% in the target plane.

2.2. *Basics: evolution of the phase and the intensity in the optical field during the propagation*

Before starting with the optical architecture, it may be useful to remember some basics one has to consider in the design of *FIS* and in the sections downstream. We have to manage properly the phase and the intensity of the optical field, to be propagated anywhere in the system with the help of Polarisation-Maintaining (*PM*) fibres and, as far as possible, to make it in an independent way. Let $E(t) = \frac{1}{2}(A(t)\exp[\mathrm{i}(kz - 2\pi f_o t)] + C)$ be the electric field in the optical wave from a single-mode oscillator, $A(t)$, C, k_o, and f_o being the optical pulse-shape, an arbitrary constant, the wave vector and the central frequency of the optical field. When the optical wave propagates, there exist some group-velocity dispersion (*GVD*) effects due to the dispersion of the optical index in silica. The dispersion coefficient $D_{(\mathrm{ps/nm/km})} = [\frac{\partial}{\partial\lambda}(\frac{1}{v_G})]_{\lambda_o}$, in the vicinity of our central wavelength [7] λ_o, is related to the actual group velocity $v_G = \frac{1}{k'(f_o)}$. With our *PM* fibres, we measured $D \approx -50$ ps/nm/km. Accounting for these definitions, it can be shown that the laser intensity $I(t) = |A(t)|^2$ in the presence of a sinusoidal phase-modulation [8] at frequency f_M takes the form:

$$I_z(t) = \left\{1 - 4\pi k''(f_o).m.f_M^2.z.\sin\left[2\pi f_M\left(t - \frac{z}{v_G}\right)\right]\right\} I_o\left(t - \frac{z}{v_G}\right) \tag{1}$$

The chromatic dispersion parameter $k''(f_o)$ in the left side factor of the expression $I_z(t)$ from (1) shows that, in the most general case, additional intensity-modulations may superimpose onto the delayed input pulse shape $I_o(t - z/v_G)$, after propagation. It must be underlined that their amplitude is proportional to the square of f_M, which will make it become more deleterious in the configuration of optical smoothing using high frequencies. They occur at the same frequency as the phase. In the situation of too elevated propagation-induced modulations, this can lead to the complete destruction of the output signal envelope $I_o(t - z/v_G)$. Nevertheless, as it will be explained below, the exclusive control of the pulse shape should be governed by external ways. So, referring (1), the only remedy to do it consists of using an external compensation of $k''(f_o)$. Similar calculations involving the influence of a non-uniform spectral transmission, namely $T(f)$, somewhere during the propagation also give evidence for other modulation effects. For example, let us consider spectral filtering and assume that the spectral transmission at the location of interest in the *FIS* can be approximated with the help of a first-order quadratic development according to $T(f) = 1 - \gamma(f - f_T)^2$. The value of the optical transmission is unity at $f = f_T$. The term γ simply involves a constant related to the spectral width of the filter. These definitions lead to another fairly simple expression of the output intensity, in the presence of sinusoidal Phase-Modulation:

$$I_z(t) = \left\{1 - 4\pi^2\gamma\left[f_T + m.f_M.\cos\left[2\pi f_M\left(t - \frac{z}{v_G}\right)\right]\right]^2\right\} I_o\left(t - \frac{z}{v_G}\right) \tag{2}$$

Both Eqs. (1) and (2) apply to spectral transmission effects on the optical wave, which involve un-equalised optical effects due to filtering, or etalons effects, as well as amplification. They provide a basic model to be used for the coupling of temporal and spectral phenomena in the presence of phase-modulation in the *FIS*. A more complete and effective analytical description would be quite more complex. These phenomena can be related to the more general *FM–AM* conversion effects, i.e., the conversion of Phase-Modulation, or Frequency-Modulation, to Amplitude-Modulation.

The *FM–AM* conversion effects due to the combination of $P_h M_{SBS}$ and $P_h M_{SSD}$ should be considered simultaneously, together with additional propagation phenomena which include depolarisation along the fibres or at the location of connectors, air-gaps, and cascaded etalons. Even though they exhibit a specific interest in the optimisation of global temporal performance, the development of completed expressions to account for all these phenomena is beyond our topic of this article. Eqs. (1) and (2) can be considered sufficient for a first insight in the area. Before we go on, we

still have to refer to the time-integrated *PSD*, denoted as $\tilde{A}(w)$. By assuming, for the sake of simplicity, a constant signal power at the input of the system in the form $A_o(t) = \exp[im\sin(2\pi f_M.t)]$, it becomes [9]:

$$\tilde{A}(f) = \sum_{-\infty}^{+\infty} J_k(m).\delta(f - kf_M) \tag{3}$$

where m and f_M are the modulation index and the frequency of the Phase-Modulation, either for *SBS* or *SSD*, while the constants $J_k(m)$ can be found in the mathematical tables to describe the Bessel distribution. Finally, the spectral width of the *PSD* in wavelength units finally gets the time-integrated enlarged value $\Delta\lambda_{\text{tot}} = 2.m.f_M.\lambda_o^2/c$. The operation of m with precisely controlled values provides an efficient tool to modulate the coherence level in the complete facility a simple way, and meet given requirements downstream of the *FIS*.

2.3. Architecture and sizing of the FIS

Now we can enter the design of the optical architecture of the system. The *FIS* (Fig. 1) will have to deliver simultaneously between 30 and 60 pulses, together with independent temporal pulse-shapes to be defined one by one in a fully arbitrary way. The front part consists of the Single-Mode oscillator, which is placed upstream of the two phase modulators to be used for the implementation of the *SBS* suppression system and the *SSD* operations. Specific diagnostics are placed just after the *SBS* block-function to verify the effectiveness of $\Delta\lambda_{SBS} > 0.15$ nm. A 100 m long fibre section provides the suitable delay to compensate for the time response of the control-electronics to address the two blocking-up downstream *AM* block-functions. Thus, the pulse can be stopped.

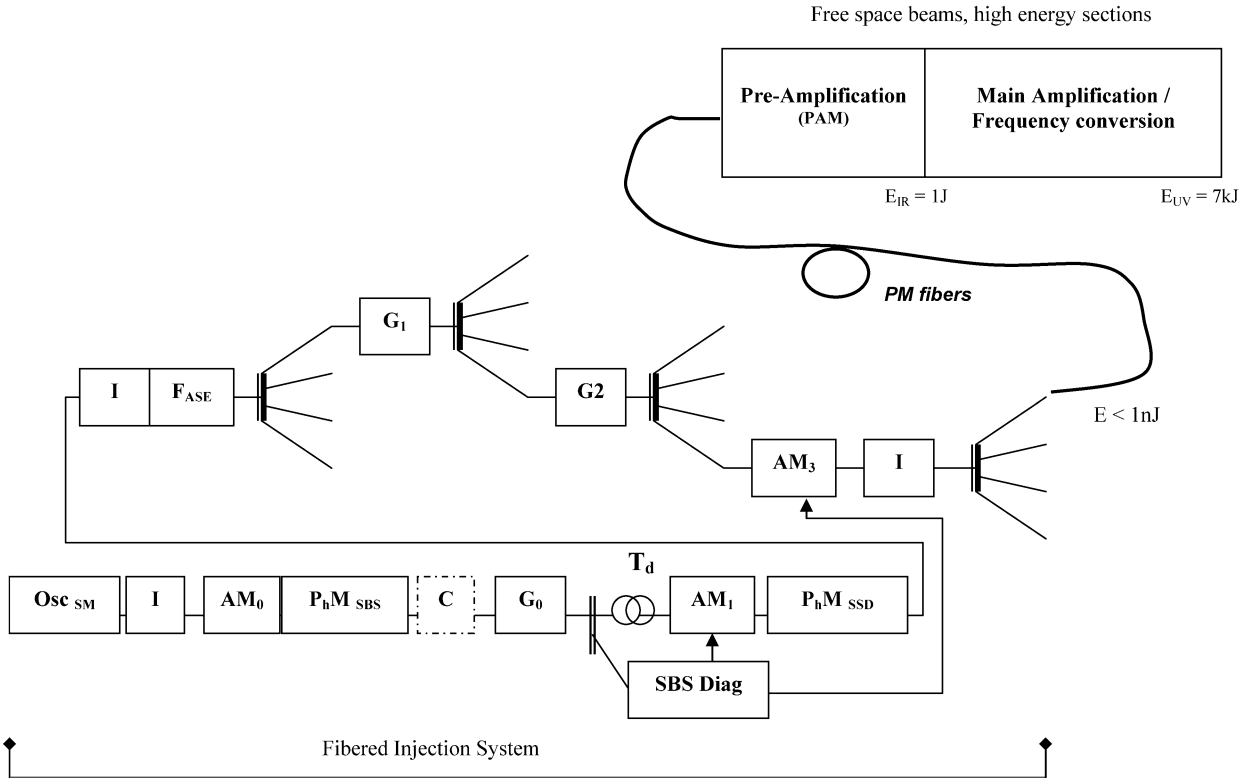

Fig. 1. The architecture of the *FIS* design on *LIL*: the single-mode oscillator (Osc_{SM}), amplitude (*AM*) and phase ($P_h M_{SBS}$ and $P_h M_{SSD}$) modulators, the GVD compensator option (*C*), the amplifiers (*G*) and specific isolators (*I*), the *PM* fibered splitters '1 to 4', the SBS diagnostics and the related delay line (T_d).

Fig. 1. Architecture du *FIS* concu pour le *LIL* : l'oscillateur monomode (Osc_{SM}), les modulateurs d'amplitude (*AM*) et de phase ($P_h M_{SBS}$ et $P_h M_{SSD}$), l'option compensateur de GVD (*C*), les amplificateurs (*G*) et les isolateurs spécifiques (*I*), les diviseurs à fibre *PM* « 1 vers 4 », les diagnostics *SBS* et la ligne à retard associée (T_d).

The injection of all the laser lines with the help of a unique oscillator guarantees the same central wavelength anywhere in the system downstream. Its value, $\lambda_o = 1053.00\ \text{nm} \pm 5\ \text{pm}$, is specified in the vacuum together with the required long-term stability. Such a huge precision helps us to control the effectiveness of the *SBS* Phase-Modulation, at the confidence level theoretically required by a proper management of lifetime of the optics in the complete *LMJ*: there should be no more than one failure every 10^{12} to 10^{15} laser shots, to avoid laser damage in the multi-kJ UV beam sections. In fact, we have to manage the reduction of *SBS* effects both across the UV optics and along the fibres of the *FIS* itself. The spectral profile of the longitudinal Brillouin gain [10,11] in the fibres exhibits a Lorentzian shape. It involves the phonon lifetime T_b in the silica of the fibres, the density ρ_o and the elasto-optic coefficient p_{12} of the material and the acoustic velocity v_a:

$$g_B(\lambda) = \frac{(2\pi T_B)^{-2}}{(\frac{1}{\lambda} - \frac{1}{\lambda_o})^2 c^2 + (2\pi T_B)^{-2}} \frac{2\pi^2 T_{B^2} n^7 p_{12}^2}{c\lambda_o^2 \rho_o v_a} \tag{4}$$

This is the reason why $g_B(\lambda_o)$ decreases rapidly with $\Delta\lambda = (\lambda - \lambda_o)$. Moreover, there exists a threshold value of the circulating optical power not to be crossed, to prevent the initiation of these effects. The threshold depends on the peak value of G_B in (4), together with the linear absorption (α), the core section (S) and the total length (L) of fibre over which the optical power is distributed:

$$P_O^{\text{th}} \approx 21 \frac{\alpha S}{[1 - \exp(-\alpha L)] g_B(\lambda_o)} \tag{5}$$

Eqs. (4), (5) help to estimate the orders of magnitude in the allowed pulse peak power versus the pulse duration P_{peak} and the pulse repetition frequency (F) for a given value of $\Delta\lambda$. It comes that P_{peak} can reach about 10 W with $F < 100$ kHz, as soon as $\Delta\lambda_{\text{tot}}$ exceeds the specified minimum value of 1 Å. The only issue for the absence of *SBS* effects in the *FIS* essentially consists in the absence of any risk of failure in the application of phase modulation, the topic which will be detailed below. Anyway, the main purpose of *SBS* suppression from the *FIS* concerns that of keeping the transverse amplification low enough inside the large UV optics [1] downstream the output of the large amplifying sections in *LIL–LMJ*. This needs to be guaranteed within transverse dimensions on the order of $40 \times 40\ \text{cm}^2$, for up to 30 ns wide pulses and output intensities in the range of $10\ \text{J/cm}^2$. The huge cost of the *UV* optics explains the need of a huge confidence in the $P_h M_{SBS}$ process. As a consequence, we have to implement highly reliable specific diagnostics inside the *FIS* for a permanent control of the effectiveness of $P_h M_{SBS}$. Their role is to prevent the injection of any un-modulated or lowly-modulated pulse downstream of the *FIS*.

The *SBS* Phase-Modulation ($P_h M_{SBS}$) is operated at $m = 7$ with $f_{SSD} = 2$ GHz, which leads to a minimum spectral width $\Delta\lambda_{\text{tot}} \sim 0.15$ nm in the facility. Apart from it, the *SSD* Phase-Modulation ($P_h M_{SSD}$) is operated at $m = 5$ with $f_{SSD} = 14$ GHz. This way, the spectral width $\Delta\lambda_{\text{tot}}$ for optical smoothing is about 0.75 nm, which corresponds to nearly 98% of the enclosed optical energy per pulse. An optical *GVD* compensator (C) based on the use of an in-line grating is placed in front of the first amplifier in the *FIS*. This device helps to compensate for the effect of $k''(f_o)$, according to the reciprocal of the expression in the right part of the related factor in Eq. (1). To be efficient, such a unique compensator obviously requires equilibrated optical paths everywhere in the *FIS*, and in the facility. This was not achieved yet on *LIL*, and a number of complementary options need to be tested before their implementation at the time of the first multi-beam experiments involving *SSD*.

The configuration of the *FIS* on Fig. 1 is consistent with the delivery of up to 64 independent outputs for pulse shaping (before AM_3 modulators). One single line in the structure is based on the cascading of four *PM* fibre-coupled splitters. The actual pulse at the output end is divided into 4 equally balanced output pulses, to be re-distributed. An isolated-Yb^{3+} doped-amplifier is placed between two splitters to compensate for the in-line optical losses, on the order of 8 dB from the input to one of the four outputs of a single splitter. Even though no more than eight outputs may be used on *LIL*, in the extreme configuration of eight independent beam-lines, we needed to be consistent with *LMJ* needs. The entire number of required splitters and amplifiers has been assembled in series for a demonstration of the overall performance to be expected with the 120 *PAMs* in the updated configuration of the *LMJ*. However, the final numbers and the output coupling towards the *PAMs* still remain options to be defined. Since, in any case, the power balance and spatial uniformity on the target imply the use of a single pulse-shaping system upstream each quad, there should remain a total of 60 pulse-shapers.

Each of the eight available outputs from the *FIS* on *LIL* delivers laser pulses of which the peak output power ranges up to 100 mW, together with pulse-shape durations in the range 0.3–25 ns. The pulse-to-pulse jitter remains lower

than 7 ps RMS and the pulse repetition frequency (F) can be adjusted from 1 to 100 kHz, typically. The pulse-shapes are sampled with a time step of which the value is 100 ps $\pm$ 1 ps. The standard profiles involve the mix of flat and Picket–Fence like areas [12], with increasing and decreasing areas over any time interval. Actually, $\Delta t = 200$ ps is the minimal value of the rising and leading edges anywhere within a given pulse. The pulse-shaping systems make use of computer-controlled electronics to drive Mach–Zehnder like Amplitude Modulators (*AM*). The AM_3 block-function dedicated to pulse-shaping on Fig. 1 make use of about 300 independent voltage samples which are delivered on the signal electrode. This enables us to cover a temporal window of 30 ns, at the required precision level. To guarantee the output performance, a given set of these 300 samples needs to account for the calibration of the complete electro-optical transfer function defined by the operating points of the *AM*.

The output block-function AM_3 is placed just before the last splitter. The insertion losses of this modulator then need to be low enough to enable the feeding of one complete quad at the suitable output peak power value. This is an important sizing feature for the simplification of the overall structure, but the lack of any fibre-coupled amplifier downstream the pulse-shapers helps reduce the total number of components and the deleterious effects of *ASE* noise at the input of the *PAMs*.

The integration of the *FIS* takes the form of a number of independent Line Replaceable Units (*LRU*). The first *LRU* in the front-end contains the oscillator, the $P_h M_{SBS}$ and $P_h M_{SSD}$ block-functions, a gating modulator (AM_0) to isolate the oscillator and prevent CW amplification from the CW pumped amplifiers downstream, together with a first high gain amplifier (G_0). The role of G_0 in the FIS is quite important: this amplifier has to compensate for most of the optical losses in the front-end part, and to deliver a flat and unique—but very clean—pulse downstream. Because of some synchronisation requirements from line to line, the width of this pulse needs to be as high as 100 ns. An optical delay line, which is made of about 100 m of *PM* fibre, is placed in series after G_0 in order to compensate for the time response of the control system (*SBS* diag.) used to monitor the spectral enlargement due to $P_h M_{SBS}$. The two *LRUs* downstream contain the *PM* splitters and the amplifiers, while the last one inside a given beam-line contains a pulse-shaping system and the output *PM* splitter. The definition of the individual *LRU* was optimised to account for the maintenance requirements: we have to make the replacement of any individual component or sub-assembly in the system as easy and fast as possible, and to simplify the periodical calibration operations. This requirement needs to be achieved anywhere inside the complete *FIS*, the structure of which using hundreds of optical components, linking parts and driving electronics devices. The input and output connectors of a given *LRU* are *PM* and they belong to the standard *APC* family to avoid deleterious back reflections. The front-end part on the bottom of Fig. 1, up to the input

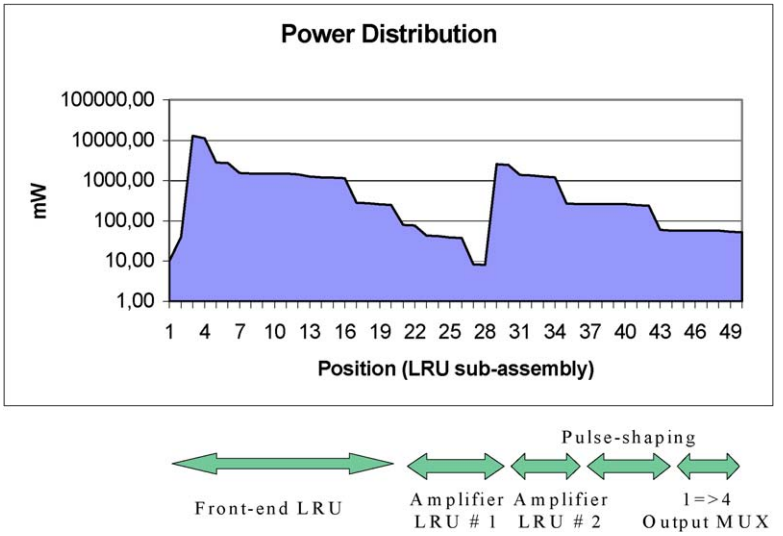

Fig. 2. A typical power budget inside the *FIS* on *LIL*: the only connectors in the system are located at the inputs and outputs of the Line Replaceable Units.

Fig. 2. Bilan de liaison typique de *FIS* sur le *LIL* : les seuls connecteurs du système sont situés aux entrées et sorties des unités interchangeables en ligne.

of the first '1 to 4' splitter, consists of the larger *LRU*. Other *LRUs* consist, respectively, of the combination of one amplifier and one splitter in the central part of the system, and the alone output splitter at the *PAM* input.

Fig. 2 indicates a typical power-budget along the single line on *LIL*, along the four *LRUs*. It makes evidence of large variations in the peak power, along the optical path from the oscillator to the *PAM*'s input: the power values range from about 10 mW up to more than 10 W.

The locations of the highest power values in the beam-lines of the *FIS* have been selected to guarantee reliable operations with the currently available components. From this point of view, we have to limit the peak power at the location of the connectors and inside the *AM* and P_hM block-functions which were shown to be the most fragile parts in the system. Since we have defined the overall structure in sufficient details, regarding the topics of optical functions and architecture, we can discuss the features and the realisation criteria of the main components used to build the different *LRU*.

3. Fibre-coupled components at 1053 nm

3.1. Wavelength generation

The oscillator (Fig. 3) is a CW device made of a standard distributed feedback structure. The Fibre Bragg Grating (*FBG*) which is deposited directly on the central part of an Yb^{3+}-doped *SM* section of fibre, a couple of centimetres long, determines the *SM* character of the laser emission at λ_o with the required precision. The active fibre is core-pumped with the help of a *SM* diode at 975 nm.

The temperature of the diode is regulated and a properly designed thermo-mechanical control of the *FBG* ensures the suitable wavelength stability. This way, the output wavelength can be adjusted as required within the spectral range ± 100 pm. The adjustment is done by mechanical or thermal means, or in combination. A mechanical device helps to control the output linear polarisation with a special care in the regards of the long term stability: this way, higher than 25 dB *PER* can be guaranteed for tens of working hours without any need of re-adjustment.

3.2. In-line signal transportation and amplification

The signal transportation between and inside the different *LRUs* is operated with the help of *SM/PM* fibres, of which the cut-off wavelength is in the order of 980 to 1000 nm. The geometry is that of *PANDA* [12], in which the rotational asymmetry leads to the separation of the orthogonal polarisation modes by the way of stress induced birefringence. The beat length, namely the ratio of the working wavelength to the index difference between the two orthogonal axes, is lower than 2 mm. Regarding the long term *PM* performance, the Polarisation Extinction Ratio (*PER*) can be kept in excess of 25 dB over 100 m, typically, with a proper alignment of the input polarisation. The diameter of the core mode is $\sim$ 6–7 μm, and the optical aperture is ~ 0.1.

In-line amplification is made with the help of Yb^{3+}-doped side-pumped fibres, using CW multimode pump-diodes of which the wavelength is 975 nm and the power can be adjusted within the range 1–2 W. The technology of side pumping makes use of the so-called V-Groove process [12], which enables the use of high power multimode pump diodes together with the lack of any discontinuity along the fibre cores. The role of the amplifiers consists in maintaining a minimal Signal to Noise Ratio (*SNR*) at critical locations inside the *FIS*. Obviously, we do know that such a design does not consist of the best configuration in the search of the attainable highest values of the *SNR*, when one

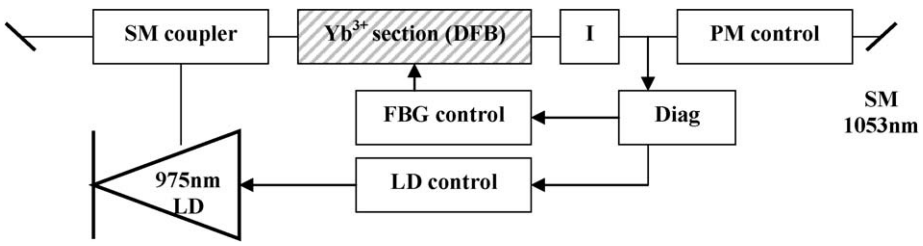

Fig. 3. The single-mode oscillator at 1053 nm.

Fig. 3. L'oscillateur monomode à 1053 nm.

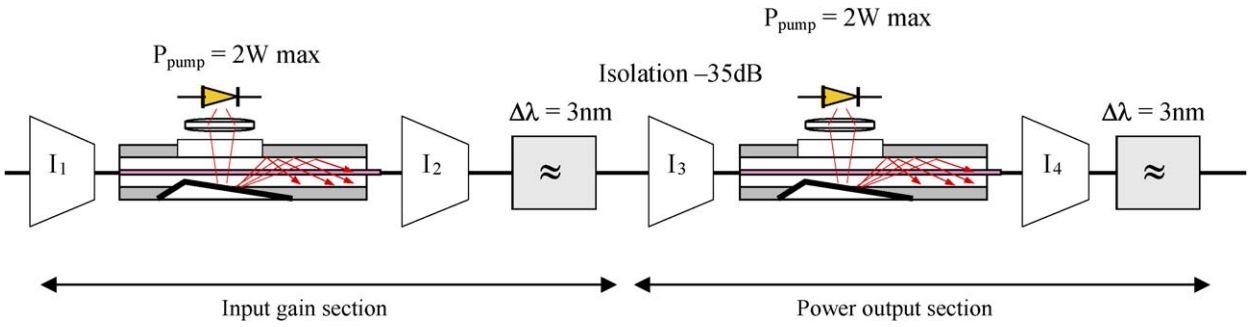

(a)

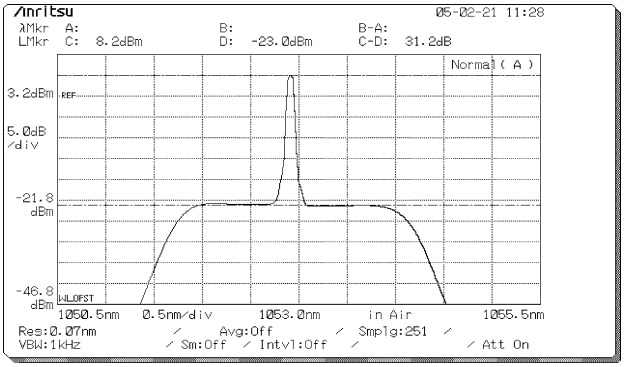

(b)

Fig. 4. Typical design of the double-clad double stage amplifiers: (a) the basic design with inter stage isolators (I_1 to I_4) and *ASE* filters (≈). The overall structure provides the single block gain function, (b) spectral output with filtered *ASE*.

Fig. 4. Architecture typique d'un amplificateur double étage à double gaine : (a) architecture de base avec isolateurs inter-étage (I_1 to I_4) et filtres *ASE* (≈). La structure globale correspond à un module amplificateur élementaire, (b) spectre de sortie avec *ASE* filtrée.

considers only the distribution of localised noise factors [5]. However, the choice of such an arborescent structure simply results from technico-economical considerations and from a particular trade-off: in a first step, the most expensive and critical block-functions need to be factorised. On another step, the best gain distribution needs essentially to be adjusted versus the power limits due to the damage effects in the components and the selected multiplexing ratio of the *PM* splitters. The characteristics of the doped sections, a few meters long, are optimised versus the laser requirements: the peak of the fluorescence needs to be not too far from λ_o and the doping level needs to be high enough to ensure an optical efficiency in the order of 80%. Regarding the *SNR* issues, it must be underlined that the aim is not the signal super-imposed noise by itself, but the remaining optical baseline noise in the output of the system. The baseline extinction essentially depends on the performance of the *AMs*. So, the design of the amplifiers is dedicated to the enhancement of *PM* capabilities more than to a specific optimisation of the *SNR*. This will be something important for the reduction of *FM–AM* conversion effects. The active area of a given amplifier consists of an Yb^{3+} doped *PM–SM* core section, which is coupled to input and output isolators. Recently, it was decided to replace the simpler one-stage devices, which were first implemented on *LIL*, by double stage devices. Despite a more complex structure, double stage amplifiers (Fig. 4) are more efficient: a complete gain-block comprises an input gain section, which produces up to 25 dB small signal gain (g_o), and an output power section to elevate the total gain by an amount of 8 to 15 dB. A couple of 3 nm wide *ASE* filters are placed at the output of both stages, to ensure a low noise accumulation along the cascaded amplifiers. The essential mean numbers to keep in mind for a complete gain-block are a minimum small signal gain $g_o \sim 30$ dB at 1053 nm, a saturation power $P_{\text{sat}} \sim 1$ W, an optical *SNR* > 17 dB in the pulsed regime and a value of the *PER* ∼ 25 dB in the long term. These values account for the effects of the backward and forward *ASE* coupling between the complete number of amplifiers in series, of which the result is a decrease in the actual net gain per block. Depending on the location of the amplifier and on the gain of the nearest other ones, the decrease in the small signal gain can vary from 1 to 2 dB for $\Delta\lambda_{\text{tot}} = 3$ nm.

The expected variations in the gain (G) and the peak output power (P_{out}) from a given amplifier during operation inside the *FIS* can be determined versus the sizing parameters [13] and a given coefficient (k):

$$\begin{cases} G \leqslant \min\left\{\exp(N_{\text{tot}}\sigma_e L),\, 1 + \dfrac{\lambda_{\text{pump}}}{\lambda_o}\dfrac{P_{\text{pump}}}{F T_p k P_{\text{in}}}\right\} \\ P_{\text{out}} \leqslant \min\left\{k P_{\text{in}} \exp(N_{\text{tot}}\sigma_e L),\, \left(1 + \dfrac{\lambda_{\text{pump}}}{\lambda_o}\right) k P_{\text{in}}\right\} \end{cases} \tag{6}$$

where the constant k stands for the former decrease in the gain. The other sizing parameters in (6) are the pump power (P_{pump}) of the amplifier under consideration, the input pulse duration and peak power (T_p, P_{in}), the length and the doping level of doped fibre (L, N_{tot}) and the emission cross section (σ_e) of Yb^{3+} at λ_o. Eq. (6) basically results from the energy conservation from the pump and from the definition of the small signal gain. They consist of the simplest way to control the operating powers anywhere in the system for a given value of F. They also help understand how to prevent the optical damage due to high peak powers, especially at the location of connectors and modulators, and preserve relevant values of the signal power. The two determinations of G and P_{out} in (6) are used to re-adjust continuously the in-line gains, in the presence of slowly variable optical losses upstream any optical node in the *FIS*. The objective values of P_{out} and G can then be estimated everywhere in the *FIS*, by considering the effective numbers related to standard amplifiers made of commercially available fibres, i.e., $\sigma_e \sim 2.5 \times 10^{-21}$ cm^2 and doping levels in the range $N_{\text{tot}} \sim 8 \times 10^{20}$ cm^{-3}: let us assume $F = 30$ KHz and $T_p = 30$ ns. The application of (6) to the example of a single stage amplifier which makes use of a total pump power of 1 W and a fibre length $L = 5$ m shows that G and P_{out} should be varied up to 40 dB and nearly 20 W when P_{in} lies in the range 10–100 mW. The theoretical maximum small signal value of G from the upper equation in (6) is about 43 dB. Such numbers only indicate orders of magnitude. Since there exist significant insertion losses in the amplifiers, because of soldering and additional losses due to the presence (Fig. 4) of additional components, the net values of related gains and powers are somewhat lower. However, effective small signal gains in excess of 38 dB are currently experienced from a double stage gain-block. To refer to the scheme of Fig. 1, the typical gains of the amplifiers at the outputs of the second (G_1) and the third splitters (G_2) are adjusted within the range 15–22 dB, while the gain of G_0 is fixed in the range 28–30 dB. The adjustment of the pump power needs to be realised very precisely inside each beam-line of the *FIS*, amplifier per amplifier, and periodical monitoring operations are required to maintain the overall output balance.

The transient saturation effects induce some pulse-shape distortions but the use of high power multimode pump diodes, up to $P_{\text{pump}} = 2$ W, help keep them rather low. The maximum pulse deformations, in the order of 5 to 15% for the square wider pulses, are compensated for with the help of the pulse-shapers downstream. This enables us to prevent from any significant reduction in the dynamic range of the pulse shapes towards the output of the *FIS*.

3.3. Pulse shaping

All the *AM* block-functions in the *FIS* make use of a single Mach–Zehnder modulator of which the frequency response covers the DC-to-5 GHz bandwidth. They are implemented onto a 2 cm long $L_iN_bO_3$ substrate, in series with a $P_h M_{SBS}$ section, and benefit from a separated bias electrode for CW adjustment of the optical extinction. One of the most difficult performance issues to deal with is the optical extinction. The search of maximal optical contrasts explains the reason why our *AMs* were manufactured with the help of the proton exchange techniques, rather than the Titanium diffusion. The process of proton exchange benefits from lower than 400 °C temperatures, which enables the realisation of a high quality planar geometry with reduced optical losses. On another step, the penetration depth of the protons is much more important than that of Titanium ions. This enables the realisation of larger guiding structures with lower optical losses, typically less than 0.1 dB/cm. But the most interesting capability of the proton exchange technology regarding our requirements consists of its basically polarising capabilities. Indeed, if the two orthogonal polarisation directions can be guided as well in the case of titanium diffusion, only one can exist with low losses when one uses the proton exchange technology. This way, values of the *PER* in excess of 60 dB can be obtained from a single interferometer. Thus, remembering that the *PER* can be written in the form $PER = -10\log(e)$ to make use of the optical extinction ratio e between the input and the output fibre, we can write the transmission transfer-function of the *AM*:

$$T = \frac{I}{I_o} = \left[\frac{1+e}{2} - \frac{1-e}{2}\cos\left(\pi\frac{V}{V\pi}\right)\right] \tag{7}$$

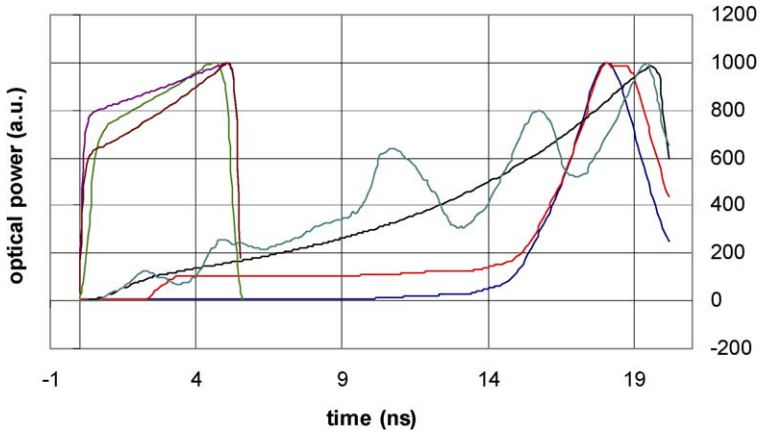

Fig. 5. A variety of measured output pulse shapes from the *FIS*: the standard profiles on *LMJ* (red, dark blue), a pure exponential (black), some shaped rising steps (brown, green, purple) and an arbitrary shape (light blue).

Fig. 5. Différentes formes d'impulsion mesurées en sortie du *FIS* : profils standards du *LMJ* (rouge, bleue foncé), forme exponentielle pure (noire), formes en créneaux (marron, vert, violet) et forme arbitraire (bleu clair).

where T equals the actual transmission for the so-called half-wave driving voltage ($V = V_\pi$). It exhibits the non-zero minimum value $T = e$ for $V = 0$, when the bias voltage has been properly adjusted. Eq. (7) accounts for the complete optical path, except the influence of misalignment between the fast axis of the input or output fibres and the plane of the wave-guides. The typical angular uncertainty is lower than ± 0.5 degree, which participates in the insertion losses. The calculation of the required precision for the electrical amplitude to be applied on the driving electrode, i.e., the variation $\frac{\Delta I}{I.\Delta V} = \frac{\pi}{V\pi} \frac{(1-e).\sin(\pi \frac{\pi}{V\pi})}{(1+e)-(1-e).\cos(\pi \frac{\pi}{V\pi})}$ from (7), leads to asymmetric bell-shaped curves of which the maximum typically ranges from a 1 to 5% per mV. This helps to put relevant numbers on the required noise performances for the driving system. The electrical *SNR* at the output of our pulse-shaping electronics exceeds 24 dB, which remains consistent with our needs. Another important feature consists of the long-term optical stability regarding the *PER* and the optical peak power. Despite some temporal variations in V_π, which come from the charge trapping effects under CW electrical polarisation [15], the *PER* is kept below -50 dB for a number of working hours. Such a performance results from the combination of the very high extinction capabilities of our *AMs* together with a properly designed feedback loop. This way, it was possible to integrate the $P_h M_{SBS}$ block-function at $f_M = 2$ GHz onto the same substrate for the reduction of the total insertion losses below 80 dB in one complete beam-line of the *FIS*. Most of the losses occur at the $L_iN_bO_3$*–SM/PM* fibre coupling areas of the modulators. The other numbers to keep in mind for the composite *AM–*$P_h M_{SBS}$ modulators are the following: ~ 6 dB insertion losses, lower than -40 dB optical back reflections, $V_\pi \sim 1$ V and 5 V on the bias and signal inputs respectively.

Fig. 5 presents a number of measured pulse shapes which have been produced with the complete pulse shaping system, including the standard shapes dedicated to *ICF* experiments on the *LMJ* (in red and dark blue). This provides an illustration of the system's flexibility.

4. Some critical design issues for the optimisation of performance

Among the numerous issues for the optimisation of the optical performance from the *FIS*, we have to notice three particular ones: the management of the hazards leading to catastrophic optical damage, the reduction of *FM–AM* conversion effects and the problem of the power output balance in the long term.

4.1. Optical damage

Regarding the hazards of optical damage in the *FIS*, two specific issues need to be designed separately: the possible failure of Phase-Modulation leading to the instantaneous damage of components and the capability of these components to be operated at very high peak powers.

Since the earlier pulses in the upstream section of the *FIS* exhibit a larger width, the highest pulse energy propagates in the front-end parts of the first *LRU*. In the situation of some instant failure in the $P_h M_{SBS}$ operation, this *LRU* also appears to be the more fragile one with respect to *SBS* effects. Due to the presence of a number of cascaded amplifiers, the *SBS* is expected to initiate from the highest source term, i.e., the *ASE* power. According to (4) and (5), the initiation of longitudinal *SBS* may occur from signal peak powers in the range of some 100 mW, depending on the involved fibre length at the initiation of the process. The induced instantaneous effects then include a strong reduction of the transmission in the fibres, or back-and-forth reflections leading to additional noise. Finally, optical damage may be experienced at the connectors or inside the modulators. Because of photo-refractive effects and other limitations, crystals made of $L_iN_bO_3$ exhibit a poor tolerance to high optical intensities, which explains why the modulators determine the most fragile locations in the *FIS*. Nevertheless, as shown in (4), the rapid decrease of the Brillouin gain in the fibres versus $\Delta\lambda_{tot}$ indicates that the effect is very simple to overcome. So, the reliability of the complete system only implies to detect the possible failure of a given $P_h M$ block-function or its driving electronics. The optimisation route for reliability is driven essentially by the principle of redundancy in the dedicated *SBS* diagnostic block-function (*SBS Diag*) of Fig. 1, and the control locations inside the *FIS*. This is the reason why this block-function addresses, simultaneously, the two independent *AMs* denoted AM_1 and AM_3 in the figure.

The *SBS Diag* itself is made of two independent detectors, to control of the effectiveness of $f_M = 2$ GHz, each of them being unique by its operating principle and the involved technology. This way, we minimise the possible inter-correlation effects in the presence of a given failure event in the Phase-Modulation. By referring to the value of T_d in Fig. 1 and the maximum pulse repetition frequency $F = 100$ KHz, the time response of the two monitoring paths is short enough to block the incoming pulse itself after any instantaneous failure event in the spectral conditioning. The first detector employs quadratic heterodyne detection, while the second one consists of pure optical filtering with the help of a specially designed *FBG*. The blocking bandwidth of the *FBG* is 100 pm and the central frequency is peaked on to that of the signal with a precision in excess of 10 pm. Such precise values enable the transmission of a fractional part of the optical power, of which the *PSD* corresponds to the highest order Bessel lines, and this fractional part is compared with to the theoretical value one must expect for the corresponding value of m. In the situation of two inconsistent values, the blocking order is provided. The heterodyne detection makes use of the conversion of 28 GHz and higher harmonics, which results from the mixing of frequencies into the Phase-Modulated signal, into a low bandwidth signal. This process can be considered as the induction of a precisely controlled amount of *FM–AM* conversion. This low bandwidth signal is provided with the help of a very fast photodiode. Using a precise calibration process, this information is compared with a threshold value. The threshold must always be crossed if one wants to prevent the activation of the two *AMs*, i.e., to enable the transmission of the faulty pulse into the last *LRU* of the *FIS*. The controlling electronics of the *SBS Diag* helps guarantee the expected value of $\Delta\lambda_{tot}$, with a precision on the spectral enlargement of the pulses in the order of 20 pm, under permanent monitoring of the two detector outputs.

The problem of the maximum peak power level permitted in the *AMs* looks more difficult to approach. If it was supposed well known, the related response should lead to the discussion of the *LRU* distribution in Fig. 1, especially the permitted maximum value of G_0 and the total number of *PM* splitters. New optima could be designed. But we suffer from the lack of any reliable specification from the manufacturers, and from completed data in the literature. Anyway, such a response needs to account for assumptions like the total number of working hours within specified conditions, and the disrupting probability of a component. Furthermore, the lack of any reliable data on the comparison of CW and high peak power pulsed operation at moderate duty cycles is another problem. Finally, the only practical consideration to use consists in making confident with a few time–limited and sample–limited measurements which were made on representative *AMs*, and to consider some safety margins. The related tests demonstrated more than 100 hours of operation without any degradation in the optical performance, up to 50 mW CW, in the area of 1 μm wavelength. Thus we consider that peak powers in the range of 5–10 W for 1–100 KHz pulse repetition frequencies should be a satisfying trade-off: our experience of the long term operations in the current versions of the *FIS*, together with the available *AMs*, indicate no major maintenance problems up to such power levels, for tens to hundreds hours of operation.

4.2. Reduction of the FM–AM conversion effects

According to the principle of Fig. 1, the *AM* and $P_h M$ block-functions should produce completely independent modulation effects. This is a basic condition to guarantee the required power balance on the target, and to minimise

the optical damage inside the UV optics at the laser output. Anyway, Eqs. (2) and (4) show that any spectral transformation during the propagation and the amplification may affect the output pulse-shape. The phenomenological reasons why there can be some coupling between the *AM* and $P_h M$ functions can be resumed in the difficulty to preserve the spectral integrity of the optical wave. The basic phenomena being the transformation of the optical spectrum encountered by the phase-modulated pulse, we distinguish: the non uniform spectral transmission of the optical components and uncontrolled etalons due to internal reflections from place to place, the depolarisation effects leading to power coupling between the two axes of *PM* fibres or inside the components, and the *GVD* along 100 to 500 m total lengths of *PM* fibre.

For a given value of $\Delta\lambda_{\text{tot}}$, the terms in factor of f_M and f_M^2 in the right parts of the parentheses of (1) and (2) provide the magnitude of the parasitic modulations due to *FM–AM* conversion. For example, if we denote $\alpha = \frac{P\max - P\min}{P\max + P\min}$ the coefficient to describe their relative amplitude, the phase dispersion effects from (2) lead to the peak value:

$$\alpha = 8\pi^2.k''(f_o).m.f_M^2.z \tag{8}$$

In this case, the parasitic modulation intensity grows as the square of the modulation frequency. We will have to compensate for the effect of $k''(f_o)$ inside the overall optical design, and optimise the components in such a way that the term $\frac{I_z(t)}{I_o(t-z/(vg))}$ does not vary a lot with t: referring to the equivalent spectral transmission related to the first factor in (2) for given values of m and γ, the solutions to the problem will require the optimisation of the single transfer-functions and spectral equalisation. The selection of high performance *PM* fibres is an important issue in the design of the *FIS*. Since they concern to uncontrolled phase-effects related to large propagation lengths, the birefringence-induced *FM–AM* conversion effects generally exhibit a part of erratic variations. The corresponding value of α is expected to vary quickly versus the operating conditions. So, the *PM* fibres have to be operated carefully in the *FIS*: the angular deviations between the input polarisation and the fast axis should not exceed 2 degrees at the connections, either the input or the output of any fibre section, anywhere in the structure, in order to preserve a *PER* in the range 20–25 dB. This is not an obvious problem to solve. However, we kept this option of *PM* fibres only, for the sake of simplicity, rather than possible other ones using combined *SM*-only and polarising fibres (*PZ*). Indeed, we also have to consider the integration issues inside the facility. The *PZ*-only fibre option looked un-relevant because of the thermo-mechanical and curvature problems with signal transportation on tens and hundreds of meters. Such fibres suffer from a high optical attenuation, in the order of 1 dB/m in the small sections we could experience. The *PM*-only configuration of the *FIS* on *LIL* permitted the demonstration of the stability and optical performances in the short term, i.e., 5 to 8 working hours. But the long term performances still remain to be demonstrated for the final *LMJ*, during many day operations and local *PZ* fibres still might of interest at some particular locations in the system.

Just like noise, the *FM–AM* conversion effects are essentially cumulative along the fibres of the *FIS*. Because they involve stationary and non stationary contributions, it is very difficult to compensate for the induced parasitic intensity modulations after they have been generated somewhere. So, we need to keep the local *PER* as high as possible anywhere. The remedies consist of the addition of high performance polarisers from place to place, high quality connectors or soldering, not too short curvature radius with bent fibre sections, the reduction of fibre lengths and a proper management of the thermal effects inside the *LRUs*. Another efficient remedy [16] consists in the alternation of fast and slow axes with cascaded *PM* sections of fibre at optimised lengths, in the different sections of the *FIS*.

The *GVD* is the simpler effect to compensate for, with the help of a unique *FBG* design or a double pass grating at the input of the *FIS*. The only assumptions for an effective global compensation involve determined and length-equalised transportation fibres, at a given modulation index. Here are the actual numbers to describe the performance of the *FIS* in the area of *FM–AM* conversion: $1\% < \alpha < 5\%$ without any $P_h M_{SSD}$, for 200 m long transportation lengths on *LIL*, at $\Delta\lambda_{\text{tot}} = 0.15$ nm. It was shown that those performances result from the integration of *PM* Yb^{3+} doped sections inside the amplifiers, the technique of axes-alternation [16] and the optimisation of selected isolators–*ASE* filtering fibre-coupled components. In the presence of active $P_h M_{SSD}$ at $\Delta\lambda_{\text{tot}} = 0.75$ nm, yet, we rather have $20\% < \alpha < 50\%$. So, the configuration of optical still remains to be optimised.

For illustration purposes in Fig. 6, we can see (Fig. 6(a)) the results of some computations regarding the *FM–AM* conversion effects and an example of the measurements (bottom, Fig. 6(b)) we performed with the help of a streak camera to monitor the intensity modulations at $f_M = 14$ GHz. The computations provide a comparison of the amplitude of the intensity modulations in the presence of the Phase-Modulation $P_h M_{SBS}$ alone (top of Fig. 6(a)),

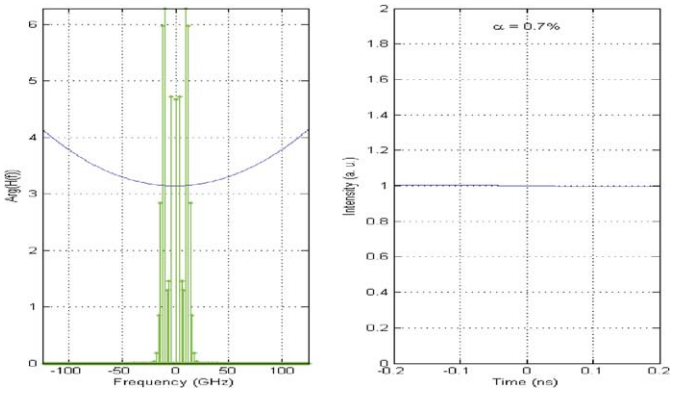

(a) $P_h M_{SBS}$ only.

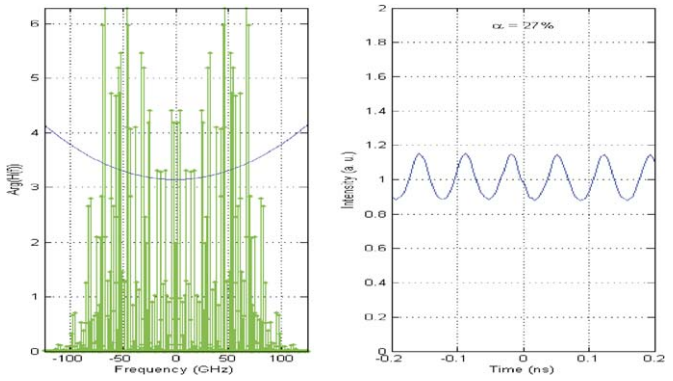

(b) Combined $P_h M_{SBS}$ and $P_h M_{SSD}$, in the configuration of optical smoothing. PSD and spectral transmission, with un-equalised devices (left panel). Output intensity modulations, superimposed on the flat input pulse shape (right panel).

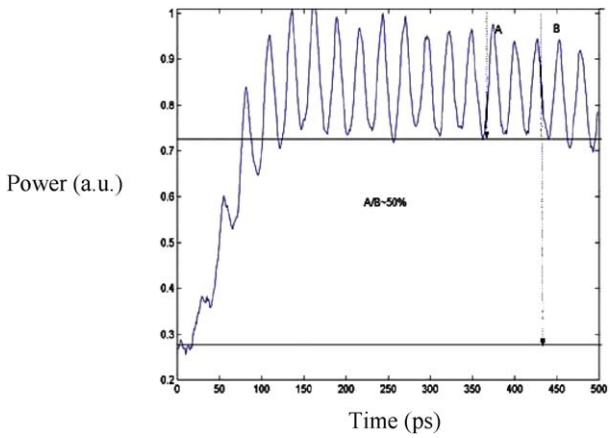

(c)

Fig. 6. *FM–AM* conversion effects at $f_M = 2$ and 14 GHz. (a) From the left to the right: the computed PSD (green) associated to the Phase-Modulated pulse with the $P_h M_{SBS}$ alone together with the assumed spectral transmission (blue), the parasitic intensity modulation at the output (blue). (b) From the left to the right: the computed PSD (green) associated to the Phase-Modulated pulse with the combined $P_h M_{SBS}$ and $P_h M_{SSD}$ together with the assumed spectral transmission (blue), the parasitic intensity modulations at the output (blue). (c) Measurements with a streak camera, to make evidence of *FM–AM* conversion effects at $f_M = 14$ GHz in the presence of $P_h M_{SSD}$ alone.

Fig. 6. Effets de conversion *FM–AM* à $f_M = 2$ et 14 GHz. (a) De gauche à droite : DSP calculée (vert) correspondant à l'impulsion modulée en phase $P_h M_{SBS}$ uniquement ainsi que le spectre transmis (bleu), la modulation d'intensité parasite en sortie (bleu). (b) De gauche à droite : DSP calculée (vert) correspondant à l'impulsion modulée en phase $P_h M_{SBS}$ et $P_h M_{SSD}$ combinées ainsi que le spectre transmis (bleu), la modulation d'intensité parasite en sortie (bleu). (c) Mesures avec une caméra à balayage de fente, pour mettre en évidence les effets de la conversion *FM–AM* à $f_M = 14$ GHz en présence de modulation de phase $P_h M_{SSD}$ uniquement.

and both the two Phase-Modulations $P_h M_{SBS}$ and $P_h M_{SSD}$ (bottom of Fig. 6(a)). For a given shape of the spectral transmission, the comparison clearly shows that the configuration of optical smoothing leads to much more important *FM–AM* conversion effects. Even though the fundamental of f_M appears clearly in both situations, the calculation of the associated *PSD* by Fourier transformation exhibits a number of higher order harmonics. The relative intensity of these harmonics may be more or less significant but, at the exception of some particular situations, the highest order harmonics are also the weakest ones. The experimental design of the intensity modulations at $f_M = 14$ GHz implies the use of an additional output amplifier, with proper spectral gain equalisation, and of a streak camera. It also implies the use of a square input pulse of which the rising time is kept as short as possible. The temporal synchronisation and the time base of this camera need to be adjusted to make the optical baseline appear (left side of the plot in Fig. 6(b)), followed by a number of modulation periods. This process enables to put numbers on the value of α from (8) by estimating the relative magnitude of the intensity modulations, with the help of the ratio of the mean peak-to-peak value in the flat part of the pulse to the mean value. This mean value is defined by the difference between the averaged power in the flat part of the pulse and the optical baseline.

5. Conclusion: the state of the art and a perspective on the possible evolutions for future *ICF* needs

The most important features of a *FIS* to be used as the laser source in large scale fusion facilities like *LMJ* has been presented, together with the experimental results on *LIL*. Today, we have designed and tested partly a fully fibre coupled design, which uses telecom-like technologies. Most of the optical performances meet the final requirements as they are known today, regarding the energies, pulse shapes, spectral distributions and long-term stability. The only remaining exception is that of the *FM–AM* conversion within an optically complex architecture. The residual modulations still need to be reduced from about 10 to 50% peak-to-peak in the *SBS*-only and *SSD* configurations, down to a few percents. The routes to reach such performances are known, and they will be experienced in the near future. They will also cross one of the most attractive capabilities of the *FIS*, i.e., the optimization of the facility's global performances from the system's input itself. In this area, the reduction of *FM–AM* conversion output contributions due to the high energy sections themselves, with the help of pre-compensation techniques in the *FIS*, is one of our forthcoming challenges.

Since this sub-system should be one of the most evolving ones in the facilities, we do not still know whether the final equipment of *LMJ* will be exactly the same. The design of the current *FIS* has been optimised for the currently required specifications and basic optical functions. But a number of evolutions could be considered. A first example consists of the capability to make the *PSD* vary during *SSD* shots. In this case, physicists either could ask for combined multiple modulations or varying m. The value of the modulation index should also vary within the pulse duration, starting from its maximum value at the beginning of the pulse and ending with reduced values during the main pulse to increase the yield of the frequency downstream, in the main section of the facility. This option of time varying spectra is not offered today in the *FIS*, but simple electro-optical solutions could be designed. Another example in the possible evolutions consists of a Picket–Fence configuration. The basic scheme of Picket–Fence is the replacement of the pre-pulse in the nominal pulse shape for *LMJ* by a series of high frequency pickets. This configuration could help to overcome the efficiency-reduced frequency conversion yield, due to the limited peak power from the large amplifiers, before the occurrence of the main pulse. Some predictions [14,17] indicate the possibility of an energy gap on the target as high as 30%. None of those new options has been analysed today, but the existing *FIS* and the fibre-coupled technologies make them quite realistic if consistent with the performance optimisation of the other sections at the highest output energy.

Acknowledgement

The authors are grateful to the CEA sub-contractors who provide their contribution to this work on *LIL*, within the framework of the *LMJ* development program at CEA/DAM. We need to thank people from the French companies IDIL and Keopsys in Lannion, Thales Laser in Orsay for the first milestones, together with people from Kentech Ltd in Great Britain and from Alenia Marconi in Italy. All of them contributed to the definition and the realization of our components and sub-assemblies, or to the integration of the complete system.

References

[1] M. André, et al., The *LMJ* prototype, in: CHOCS 29, Revue Scientifique et Technique de la Direction des Applications Militaires, avril 2004, pp. 6–11.
[2] E.I. Moses, et al., The national ignition facility: The world's largest optics and laser system, in: Proc. of SPIE, vol. 5001, Optical Engineering at the Lawrence Livermore National Laboratory, 2003, pp. 1–15.
[3] P.J. Wisoff, et al., *NIF* injection laser system, in: Proc. SPIE, vol. 5341, Optical Engineering at the Lawrence Livermore National Laboratory, 2003, pp. 146–155.
[4] A. Jolly, et al., L'injection du faisceau : le pilote, in: CHOCS 29, Revue Scientifique et Technique de la Direction des Applications Militaires, avril 2004, pp. 32–40.
[5] A. Jolly, et al., Front-end sources of the *LIL–LMJ* fusion lasers: progress report and prospects, J. Opt. Engrg. 42 (5) (2003) 1427–1438.
[6] L. Videau, et al., Le lissage optique, in: CHOCS 29, Revue Scientifique et Technique de la Direction des Applications Militaires, avril 2004, pp. 24–31.
[7] F. Devaux, et al., Simple measurement of fiber dispersion and of chirp parameter of intensity modulated light emitter, J. Light. Tech. 11 (12) (Decembre 1993) 1937–1940.
[8] L. Videau, Etude théorique de l'effet *FM–AM*, in: Note Interne CEA/CESTA/DLP/SCSL/LPL DO9 du 04/02/00.
[9] W.K. Marshall, A. Yariv, Spectrum of the intensity of modulated noisy light after propagation in dispersive fiber, IEEE Phot. Tech. Lett. 12 (3) (March 2000) 302–304.
[10] G.P. Agrawal, in: P.F. Liao, P.L. Kelley (Eds.), Nonlinear Fiber Optics, Academic Press, Inc., 1989, pp. 262–271.
[11] G. Canat, et al., 100 μJ generation using a narrow linewidth Er^{3+}–Yb^{3+} doped fiber MOPA and its modelling, in: CLEO'05, Baltimore, 2005, paper JWB67.
[12] L. Goldberg, Method and apparatus for side pumping an optical fiber, patent n° WO 97/21124 (1997).
[13] E. Desurvire, in: Erbium-Doped Fiber Amplifiers—Principles and Applications, Wiley–Interscience, J. Wiley & Sons, 2002, p. 12.
[14] J.E. Rothenberg, Ultrafast picket fence pulse trains to enhance frequency conversion of shaped inertial confinement fusion laser pulses, Appl. Opt. 39 (36) (December 2000) 6931–6938.
[15] F.T. Stone, Performance and reliability of lithium niobate integrated optical devices, in: SPIE, vol. 992, 1988, pp. 230–239.
[16] D. Penninckx, N. Beck, Axis alternation for signal propagation over polarisation-maintaining fibres, IEEE Phot. Tech. Lett., submitted for publication.
[17] The smoothing performance of ultrafast pickets on the NIF, in: Rochester-LLE Review, vol. 86, pp. 79–91.